Anal. Bioanal. Electrochem., Vol. 12, No. 3, 2020, 301-317

Analytical & Bioanalytical Electrochemistry

2020 by CEE
www.abechem.com

Review

A Review on the Semiconducting Behavior of Passive Films Formed on Mg Alloys by Mott–Schottky Analysis

Arash Fattah-alhosseini,* **and Kazem Babaei**

Department of Materials Engineering, Bu-Ali Sina University, Hamedan 65178-38695, Iran

*Corresponding Author, Tel.: +988138292505; Fax: +988138257400

E-Mail: a.fattah@basu.ac.ir

Received: 31 January 2020 / Accepted with minor revisions: 10 March 2020 /

Abstract- Mg alloys have a vast usage where weight reduction is really significant since they do the features really well for materials of ultra-light weight. However, Mg is inherently a reactive metal and its alloys generally possess quite weak corrosion resistance that widely restricts their technological usages, especially in some rough service conditions. Despite, many investigations on the passive and electrochemical properties of Mg alloys and their relation with the microstructure of these alloys, few reports have been devoted to investigate the semiconducting behavior of the formed oxide layers on these alloys. Mott–Schottky measurement is a major in-situ technique to analyze semiconductor behavior of passive layers. In this review, the semiconducting properties of formed passive layers on Mg alloys (AZ91D, AZ31B, AZ80, Mg-Y-Rare Earth-Zr alloys) by Mott–Schottky measurement has been assessed. Mott–Schottky measurements revealed the formed passive films on Mg alloys show mainly n-type behavior regardless the microstructure, pH, immersion time, and temperature of electrolyte.

Keywords- Semiconducting behavior; Mg alloys; Passive film; Mott–Schottky (M–S) analysis

---

1. INTRODUCTION

Corrosion protection against some metals and their alloys is done via the growth of passive layers in aqueous electrolytes [1–3]. This surface property is required in order to make tolerable progressions in many applications and industries where metallic components are used. Passive layers do not mostly surpass a few nanometers of thickness at ambient temperature [4–6]. Passive layers are great adherent and efficiently detach the substrate from the aggressive ambience. However, passive layers are keen to localized corrosion in the presence of aggressive species [7–10]. The passive current density of many reactive transition metals including Fe, Ni, Cr and their alloys which are faced with aqueous media is of the order ~0.01−1.0 $\mu A.cm^{-2}$ [6,11]. The really complex passivation phenomena could be affected by some factors like alloy composition, the conditions of formation and the ambience characteristics [12]. Oxide passive films which were grown on surfaces of metals and alloys have been highly studied [4,13,14]. Magnesium and its alloys have got an extensive utility in a lot of uses where reduction of weight is really important as they do the features really well for materials of ultra-light weight structural like high special strength, low density, great castability, machinability and damping features [15–25]. Nevertheless, Mg is inherently a reactive metal and its alloys normally possess quite weak corrosion resistance that highly limits their technological usages, particularly in several rough service conditions [26-30].

Based on the Pourbaix (E-pH) diagram of Mg, it can be seen that Mg corrodes over a wide range of pH and potential. In fact, the main disadvantage of Mg alloys is their low corrosion resistance that is normally; much lower while comparing with many other competing metals and alloys, such as steels or aluminum alloys [19,31]. However, the surface layer is protective at high pH (more than 11), in the area specified as passive [32].

A lot of investigations about the passive properties of Mg alloys in alkaline electrolytes have been carried out recently [33]. Mott–Schottky (M–S) test depicted that the created passive layer on magnesium alloys, presents semiconducting properties on account of its non-stoichiometric nature [18]. In spite of the widely published papers about the passivity of Mg alloys, little data about the semiconductive properties of the created passive layer on Mg alloys was accessible.

2. M–S ANALYSIS

M–S test has been shown to be an important analysis for studying semiconductor behaviors of passive layers. This test has been mainly used to evaluate the passive layers semiconducting behavior like the passive layers on Cu and its alloys [34–51], Ni and its alloys [52–62], Al and its alloys [63–69], Ti and its alloys [70–80], Ta and W [81–88], Cr [89–91], Zn and its alloys [92–95], Zr and its alloys [96–98], Fe and carbon steels [99–104] and stainless steels [10,105–115]. Based on the point defect model (PDM) [13,116–119], the defects are cation and oxygen vacancies, and cation interstitials in the passive layer. It is discussed that cation interstitials and oxygen vacancies are electron donors, resulting in n-type doping as cation vacancies are electron acceptors and consequently, doping the barrier layer p-type.
M–S test is a strong method in order to analyze the semiconductive properties of passive layers on metals or their alloys [37,47,48,120–122]. M–S relations that are used to evaluate

semiconductor type of the passive layers and the dopant density, are [8,9, 111, 123]:

$$\frac{1}{C^2}=\frac{2}{\varepsilon\varepsilon_0 eN_D}\left(E-E_{FB}-\frac{kT}{e}\right) \quad \text{n-type behavior} \tag{1}$$

$$\frac{1}{C^2}=-\frac{2}{\varepsilon\varepsilon_0 eN_A}\left(E-E_{FB}-\frac{kT}{e}\right) \quad \text{p-type behavior} \tag{2}$$

where N_D is the donor density, N_A shows the acceptor density, ε stands for the passive layer dielectric constant (ε=9.6 [15,16]), ε_0 is the vacuum permittivity, and E_{FB} presents the flat-band potential [8,9,111,123]. Table 1 indicates the magnesium and its alloys semiconducting properties.

3. SEMICONDUCTING PROPERTIES OF AZ91D Mg ALLOY

M–S curves of the solution annealed (SA) and as-cast AZ91 Mg alloy samples obtained after 1, 7, 14 and 21 days of immersion in borate buffer solution having pH of 9.2 are indicated in Fig. 1 [16]. From the M–S plots it is realized that the semiconductor behavior of the oxide layers on the SA and as-cast samples changes varies with time. It is observed that the acquired plots for 24 h of immersion show a negative slope from -1.2 V_{SCE} downward to more cathodic potentials. This change in the capacitance with the employed potential is a kind of p-type behavior.

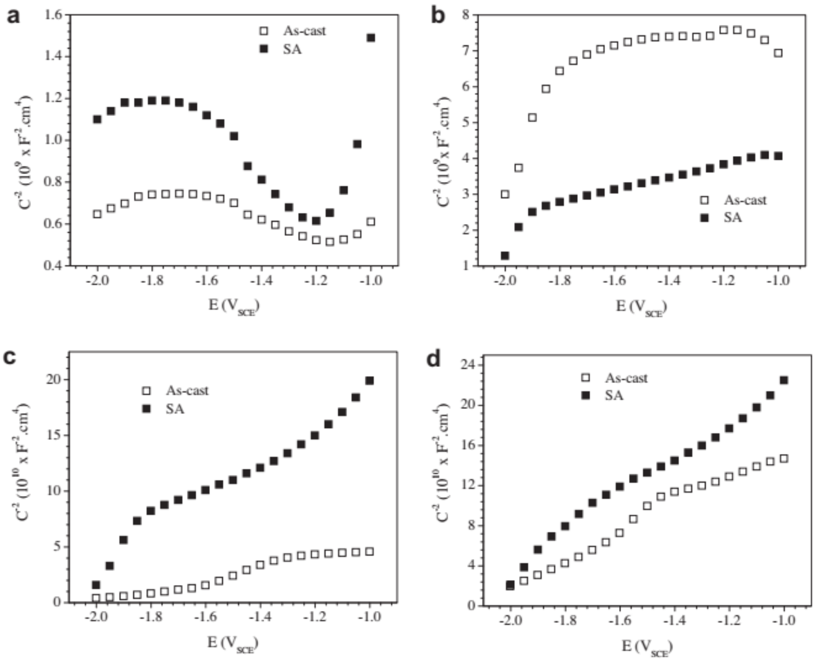

Fig. 1. M–S curves of the SA and as-cast AZ91D Mg alloy samples in borate buffer solution after different immersion immersions: (a) 1, (b) 7, (c) 14, and (d) 21 days [16]; Reprint with permission from Ref. [16] (License Number: 4758170050435, License date: Jan 29, 2020)

Table 1. The semiconducting properties of Mg alloys

Mg Alloys	**Solution**	**Semiconducting behavior**	**Year**	**First author [Ref.]**
AZ91D	Sodium borate solutions (pH=9.2)	Effect of anodic oxidation on the corrosion performance of AZ91D in borate solution reveals that higher anodizing potentials, induce better protection due to formation of rather thicker and more resistive n-type semiconducting surface films with high anti-corrosion properties	2011	El-Taib Heakal [15]
AZ91D	0.05 M H_3BO_3 + 0.075 M $Na_2B_4O_7.10H_2O$ (pH=9.2)	M–S plots showed that semiconducting behavior of oxide films changed from p-type after 1 day of immersion to n-type for longer periods for both the as-cast and solution annealed specimens	2013	Lopes de Oliveira [16]
AZ31B	0.01 M NaOH	M–S analysis revealed that passive films displayed n-type semiconductive characteristics, where the oxygen vacancies and interstitials preponderated. Based on M–S analysis, it was shown that calculated donor density (N_D) increases linearly with increasing formation potential	2014	Fattah-alhosseini [18]
AZ31B	NaOH solutions	M–S results showed that N_D are in the range of 10^{20} cm^{-3} and decreased with decreasing NaOH concentration	2014	Fattah-alhosseini [19]
AZ31B	0.01 M NaOH	M–S analysis showed that the semiconducting characteristic of AZ31B Mg alloy with and without MAO coatings displayed n-type behavior	2015	Fattah-alhosseini [20]
AZ31B	0.05 M NaOH	M–S results showed that N_D are in the range of 10^{21} cm^{-3} and increase with increasing chloride concentration	2015	Fattah-alhosseini [21]
AZ31B	0.01 M KOH	M–S results showed that N_D increases by increasing immersion time from 1 to 6 h, while it decreases when immersion time reaches 9 and 24 h	2015	Fattah-alhosseini [22]
AZ31B	0.01 M NaOH	M–S analysis indicated that the semiconducting behavior of AZ31B Mg alloy with and without MAO coatings displayed the n-type behavior	2016	Sabaghi Joni [23]
AZ80	Phosphate buffer solutions	M–S analysis revealed that passive films displayed n-type behavior and N_D increased with increasing the pH from 10.69 to 13.05	2016	Fattah-alhosseini [24]
Mg-Y-RE-Zr	Phosphate buffer solutions	M–S analysis revealed that the formed passive layers on Mg-Y-RE-Zr alloy behaved as an n-type semiconductor. An increase in N_D accompanying solutions of higher alkalinity is thought to result in the formation of a less resistive passive layer	2018	Fattah-alhosseini [25]
EV31A	0.1 M NaOH	M–S results pointed out that light illumination induced surface defects of n-type character	2018	Ninlachart [17]
AZ31B	0.01 M NaOH (pH=12)	M–S measurements showed the formed passive film on AZ31B magnesium alloy indicates an n-type semiconducting characteristics regardless the immersion time and electrolyte temperature, and the figured N_D rises exponentially by increasing solution temperature and immersion time	2019	Sabaghi Joni [33]

Zhang et al. [124] indicated that adsorbed hydrogen on the magnesium surface of can lead to a semiconducting behavior p-type, making vacancies of Mg in the oxide film that would be the main charge carriers in the layer. The identical authors published that an identical properties was seen for AZ91D [125]. Gas bubbles of Hydrogen erupted while dissolution of SA and as-cast samples up to first immersion day. The observed p-type semiconductor properties in the corresponding M–S curves (Fig. 1a) is a result of the produced hydrogen bubbles within the primary corrosion procedure of AZ91D. As more compact and a thicker oxide layer that developed with time, the progress of gas bubbles stopped. As a result, the hydrogen gas adsorption on the electrodes surface was no longer feasible. Thus, the M–S plots slope got positive from 7 up to 21 immersion days showing that the semiconducting properties of the oxide layer was changed to that of an n-type behavior [126]. Both SA and as-cast samples were imagined as the n-type semiconductor properties. For this kind of properties, anion vacancies or cation interstitials are the principal defects in the oxide layer. Duan et al. [127] saw that the oxide film on AZ91 indicated an n-type semiconductor properties while immersing within a solution of 0.1 M $Na_2B_4O_7.10H_2O$+ 0.05 M NaCl. Heakal et al. [15] have discovered a behavior of n-type for the produced oxide layer on AZ91 while immersing in a solution of borate.

Provided that the oxide layer acts as an p- or n-type behavior, the same acceptors (vacancies of magnesium) or donors (mostly vacancies of oxygen) is calculated using the slope of the linear part in the M–S curves. This density is correlated with the number of defects within the layer. A high doping concentration is same as a defective oxide film that in turn is related with a lower corrosion behavior [105]. The concentrations of charge carrier related to the average values of three distinct samples that were tested in each condition are indicated in Table 2.

Table 2. Charge carrier concentration in the oxide layer formed on the as-cast and solution annealed (SA) AZ91D Mg alloy samples in 0.075 M $Na_2B_4O_7.10H_2O$ + 0.05 M H_3BO_3 solution after different periods of immersion [16] (With permission from Ref. [16]; License Number: 4758170050435, License date: Jan 29, 2020)

Condition	**N_q (cm^{-3})** **Immersion (days)**			
	1	7	14	21
As-cast	$2.91\times10^{22} \pm 3.84\times10^{20}$	$1.83\times10^{22} \pm 2.63\times10^{20}$	$2.90\times10^{20} \pm 9.40\times10^{17}$	$1.06\times10^{20} \pm 3.07\times10^{18}$
SA	$1.21\times10^{22} \pm 1.40\times10^{20}$	$8.50\times10^{21} \pm 1.24\times10^{20}$	$9.95\times10^{19} \pm 3.20\times10^{17}$	$8.14\times10^{19} \pm 1.31\times10^{18}$

The concentrations of the highest charge carrier were discovered after 24 h. Based on Carmezim et al. [128] it is an obvious sign of a very disordered oxide layer. As mentioned before, the oxide film behaved like a p-type behavior after immersing for 1 day. So, the defects are mostly vacancies of cation. According to Table 2, the number of defects persistently declined with time for the SA and as-cast samples. In longer immersion, the oxide layer indicated an n-type behavior. Cation interstitials and vacancies of oxygen are the principal defects in this condition, behaving as electron donors. It has been related that the existence of such doping species in the oxide layer prevents the cations migration from the materials underneath the oxide film. Similar condition happens with the penetration of aggressive anions from the solution like Cl^- and SO_4^- [129]. So, the corrosion resistance will augment while the oxide film semiconducting behavior alters from p-type to n-type. The decrease in the number of defects within the oxide layer with time was shown in Table 2 and also the points to form more protective oxide films and less conductive.

4. SEMICONDUCTING PROPERTIES OF AZ31B Mg ALLOY

Fig. 2a indicates the M–S curves of AZ31B alloy in 0.01 M sodium hydroxide at selected potentials.

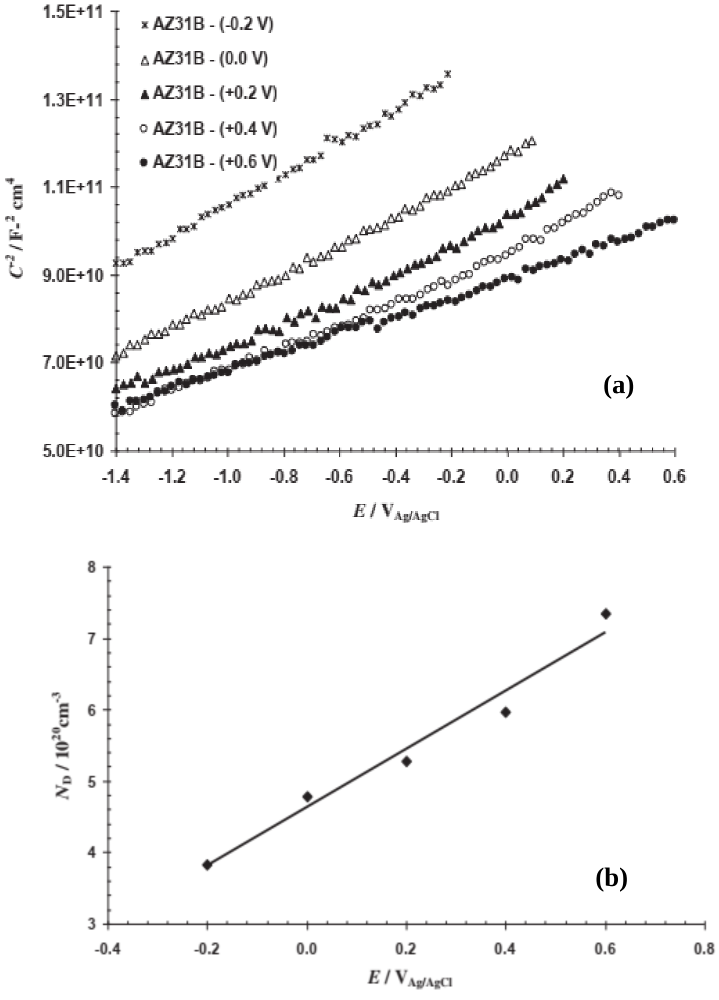

Fig. 2. (a) M–S curves and (b) N_D of the passive layer produced on AZ31B Mg alloy in 0.01 M sodium hydroxide solution at different potential [18]

As can be observed, C^{-2} obviously declines with rising the formation potential [18]. In these plots, the positive slopes are ascribed to behavior of n-type. Fig. 2b indicates the N_D of the formed passive layer on this alloy in 0.01 M sodium hydroxide [18]. The magnitude orders are about 10^{20} cm^{-3} and rises linearly with the potential. The values are similar to the N_D of the produced passive layers on AZ31B in solutions of NaOH [18,19]. Based on the PDM [118,119], the oxygen vacancy flux and cation interstitials is necessary to the growth process of layer.

Fig. 3a reveals the M–S curves of the passive films produced on AZ31B in solutions of NaOH [19]. It should be noticed that capacitances obviously decline with concentration of solution. Also, all curves indicate one zone. Fig. 3b reveals the N_D as a function of electrolyte concentration. It can be seen that the N_D obtained from plots of M–S are in the range of 10^{20} cm^{-3} and declined by declining concentration of NaOH [19].

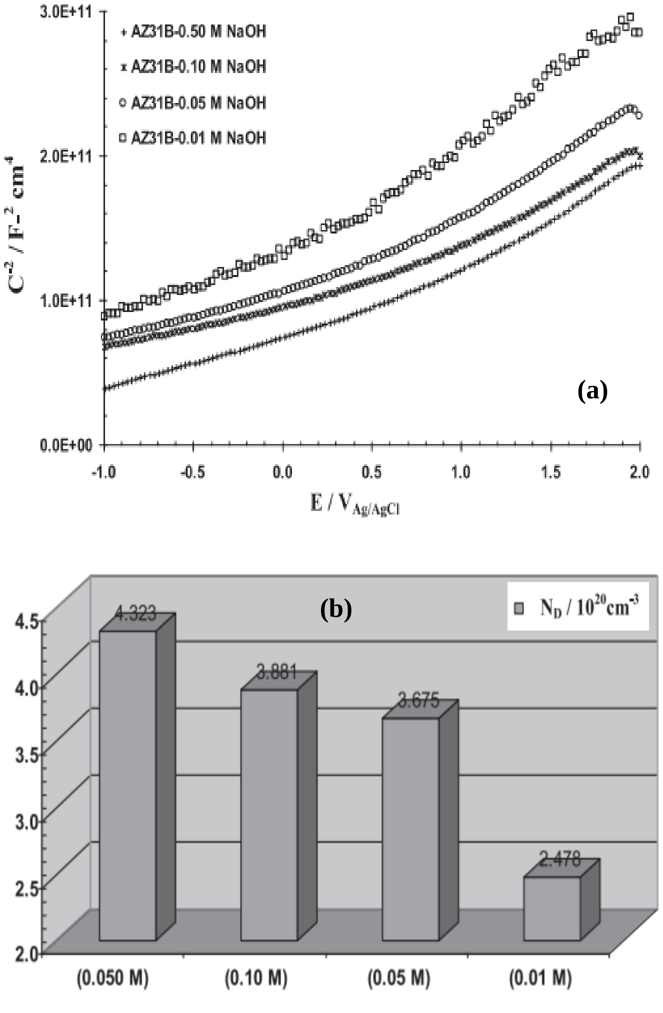

Fig. 3. (a) M–S curves and (b) N_D of the passive layers produced on AZ31B alloy in sodium hydroxide solutions [19]

Fig. 4a shows the plots of M–S for the passive films formed on AZ31B in 0.01 M potassium hydroxide [22]. All plots present one zone. Thus, this measurement depicted that the produced passive films on AZ31B indicate n-type semiconducting behavior. The obtained N_D shows the oxygen vacancies concentrations are considered to be the most. Fig. 4b shows the obtained N_D as a function of immersion time. It can be seen that the N_D of AZ31B rise by augmenting the immersion time from 1 to 6 h, whereas it declines as the immersion time attains 9 and 24 h [22].

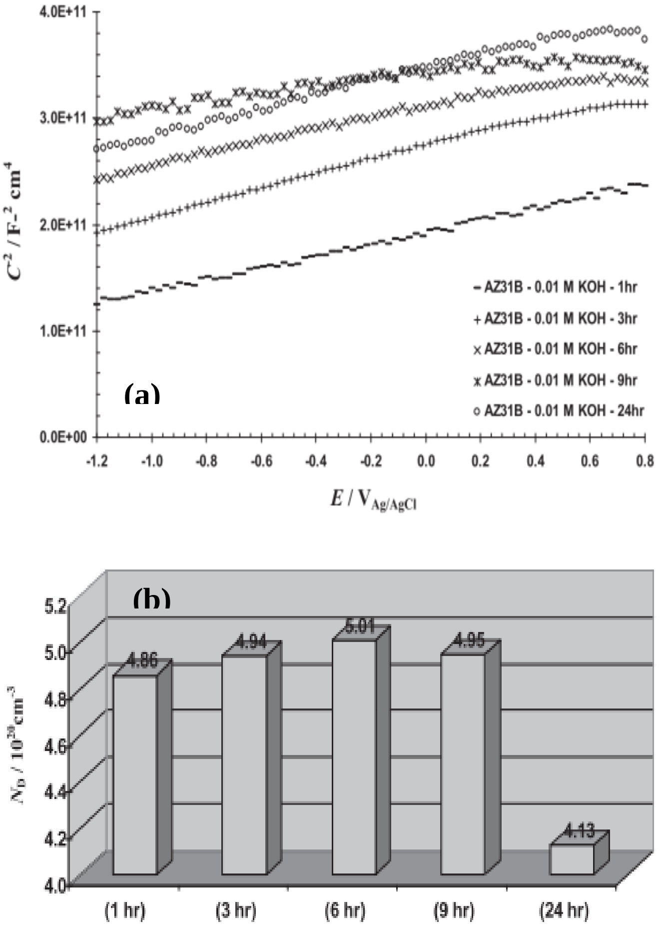

Fig. 4. (a) M–S curves and (b) calculated N_D of passive layer formed at various immersion times on AZ31B in 0.01 M potassium hydroxide [22]; Reprint with permission from Ref. [22] (License Number: 4758040563033, License date: Jan 29, 2020)

Fig. 5 reveals the plots of M–S for the passive layers produced on AZ31B in 0.01 M sodium hydroxide at 65, 45, 25 and 5 °C in various immersion times [33]. It is observed that all of the capacitance values increased by formation potential. According to Fig. 5, the decline in the slopes with the increment in temperatures of solution means an increase in N_D [33].

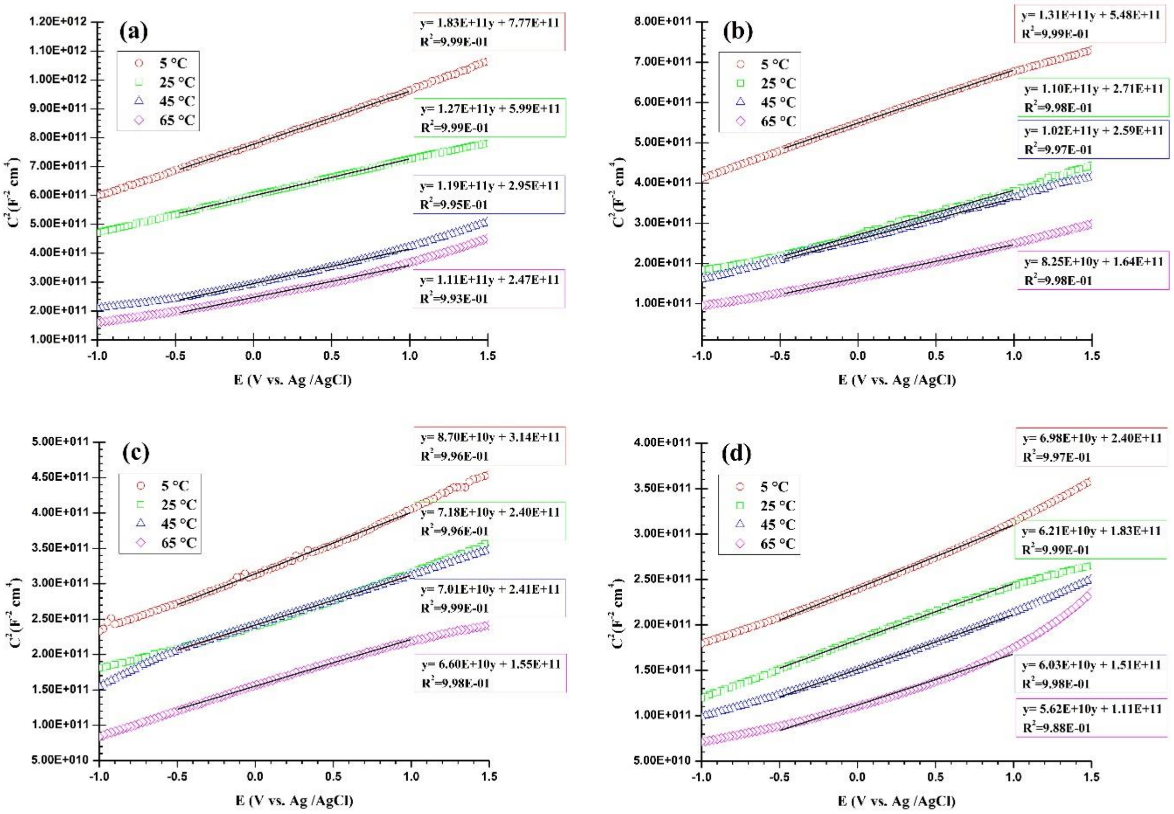

Fig. 5. M–S plots of AZ31B at various temperatures in 0.01 M potassium hydroxide after different immersion times: (a) 1200, (b) 2400, (c) 4800, and (d) 7200 s [33]

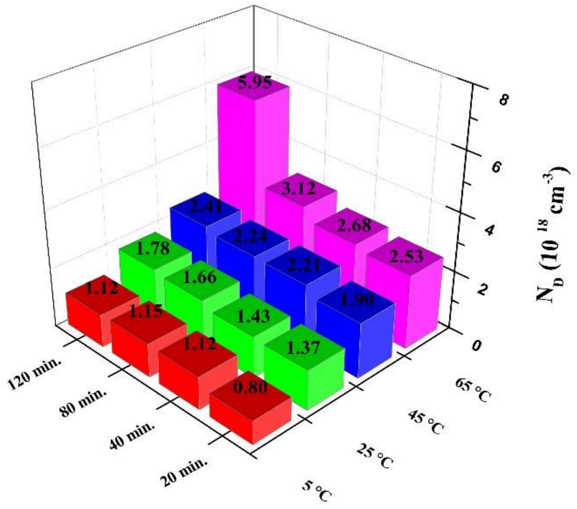

Fig. 6. The concentration of N_D as a function of immersion time and solution temperature [33]

The layer has MgO and the magnesium oxidation reaction has more inclination at higher temperatures. In other words magnesium oxidation might be assumed as a substitute for Mg^{2+} inside the passive film which can make ionic species having cation within vacancies of oxygen or interstitial sites. It can be observed that at a constant temperature by increasing the immersion time, the slopes of M–S straight lines will decline, showing an increase in N_D. On the other hand, the M–S analysis of passive behavior of Fe and Ni showed that the doping density declined by increasing immersion time [130,131]. For AZ31B, prolonged immersion time sounds to favor the absorption of H_2O using the passive layer and H_2O in a layer of n-type may function as the donor impurities because of the increment in hydration of the passive layer [132,133]. The density of donors as a function of electrolyte temperature and immersion time are shown in Fig. 6. It is observed that the magnitude orders are about 10^{18} cm^{-3}. Such high N_D showed a highly nature of disordered passive layer on AZ31B [33].

5. SEMICONDUCTING PROPERTIES OF AZ80, Mg-Y-RARE EARTH (RE)-Zr ALLOYS

Fig. 7a illustrates the plots of M–S for Mg alloy of AZ80 in phosphate buffer solutions with various pHs [24].

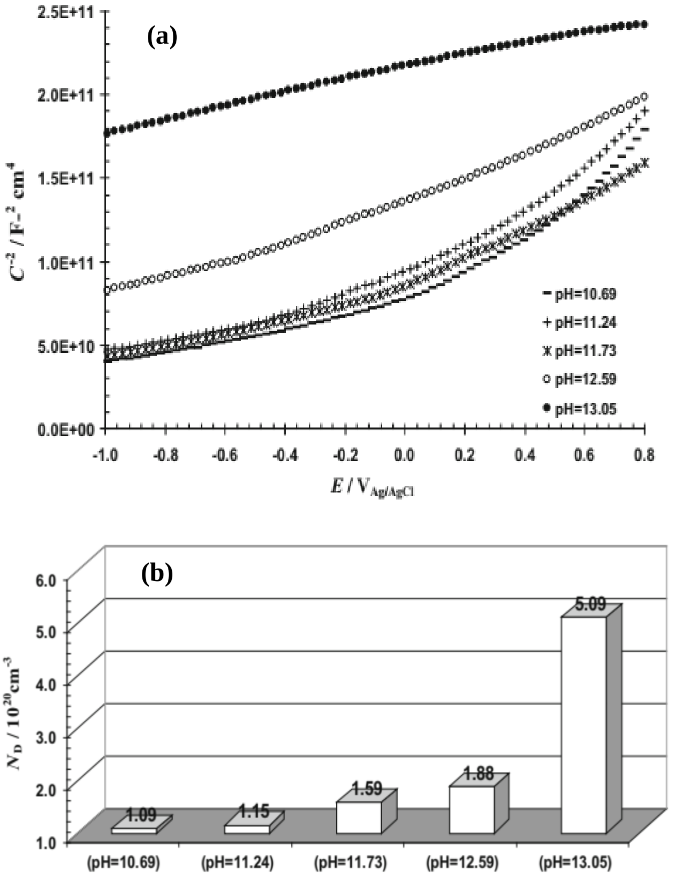

Fig. 7. (a) M–S plots and (b) calculated N_D of the passive layers produced on AZ80 in phosphate buffer solutions [24]; Reprint with permission from Ref. [24] (License Number: 4758041121805, License date: Jan 29, 2020)

All plots indicate one zone same as that mentioned formerly for AZ31B in solutions of NaOH [19]. The positive slope in this zone is ascribed to the behavior of n-type. The N_D was analyzed using Eq. (1) indicates the N_D where the oxygen vacancies concentrations and metal interstitials are considered to be the most [19,24]. Fig. 7b indicates the N_D as a function of solution pH. It is seen that the N_D augmented by rising the pH from 10.69 to 13.05.

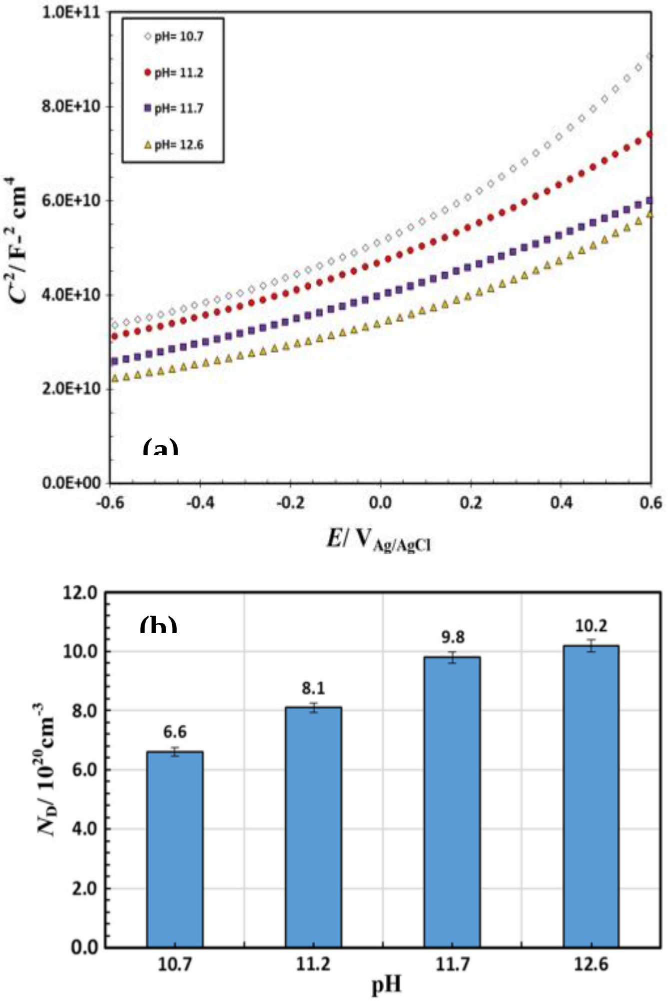

Fig. 8. (a) M–S curves and (b) N_D of passive film formed on Mg-Y-RE-Zr in phosphate buffer solutions [25]; Reprint with permission from Ref. [25] (License Number: 4758360343963, License date: Jan 29, 2020)

Fig. 8a indicates the M–S curves of the Mg-Y-RE-Zr alloy within solutions of phosphate buffer with different pHs [25]. As it is observed, this alloy indicates n-type semiconductor properties for all values of pH. Fig. 8b illustrates the comparison of the N_D as a function of the pH. As can be observed, the N_D of the passive film augments with the increment in solution alkalinity. This result displays that the higher N_D causes the passive film be more defective and, so, less resistive against corrosion [25].

6. CONCLUSION

The semiconducting behavior of produced passive layers on Mg alloys (AZ91D, AZ31B, AZ80, and Mg-Y-RE-Zr alloys) by M–S analysis is reviewed in this study. M–S measurement revealed that the passive layers mainly behave as n-type behavior. For AZ91D Mg alloy, the M–S plots indicated that the semiconductor properties of the oxide layers altered from p-type after 24 h of immersion to n-type for longer time for both solution annealed and as-cast samples. The M–S analysis divulged that the layers grown on AZ31B, AZ80, and Mg-Y-RE-Zr alloys are obviously n-type semiconducting behavior. For AZ31B alloy, in a constant immersion time, the N_D had a gradual trend for the density to augment with the increase in the temperature of solution due to a less protective layer formation. Moreover, for a constant temperature of solution, rising immersion time can make M–S curves slopes decreasing, the higher immersion time, the lower M–S curves slopes.

REFERENCES

[1] V. Maurice, and P. Marcus, Prog. Mater. Sci. 95 (2018) 132.

[2] F. Presuel-Moreno, M.A. Jakab, N. Tailleart, M. Goldman, and J.R. Scully, Mater. Today. 11 (2008) 14.

[3] U. Stimming, Electrochim. Acta. 31 (1986) 415.

[4] V. Maurice, and P. Marcus, Electrochim. Acta. 84 (2012) 129.

[5] V. Maurice, and P. Marcus, Curr. Opin. Solid State Mater. Sci. 22 (2018) 156.

[6] A. Fattah-alhosseini, and K. Babaei, Anal. Bioanal. Electrochem. 11 (2019) 1747.

[7] A. Fattah-alhosseini, A. Saatchi, M.A. Golozar, and K. Raeissi, Electrochim. Acta. 54 (2009) 3645.

[8] A. Fattah-alhosseini, M.A. Golozar, A. Saatchi, and K. Raeissi, Corros. Sci. 52 (2010) 205.

[9] A. Fattah-alhosseini, F. Soltani, F. Shirsalimi, B. Ezadi, and N. Attarzadeh, Corros. Sci. 53 (2011) 3186.

[10] A. Fattah-alhosseini, Arab. J. Chem. 9 (2016) S1342.

[11] A. Veluchamy, D. Sherwood, B. Emmanuel, and I.S. Cole, J. Electroanal. Chem. 785 (2017) 196.

[12] N.E. Hakiki, Corros. Sci. 53 (2011) 2688.

[13] D.D. Macdonald, Pure Appl. Chem. 71 (1999) 951.

[14] A. Fattah-alhosseini, M. Naseri, and K. Babaei, Anal. Bioanal. Elecrochem. 11 (2019) 1353.

[15] F. El-Taib Heakal, A.M. Fekry, and M. Abd El-Barr Jibril, Corros. Sci. 53 (2011) 1174.

[16] M.C.L. de Oliveira, V.S.M. Pereira, O.V. Correa, N.B. de Lima, and R.A. Antunes, Corros. Sci. 69 (2013) 311.

[17] J. Ninlachart, and K.S. Raja, Effect of light illumination on the corrosion behavior of Mg-RE alloy EV31A in chloride-alkaline solutions, ECS Trans. 85 (2018) 567.

[18] A. Fattah-alhosseini, and M. Sabaghi Joni, J. Magnes. Alloy. 2 (2014) 305.

[19] A. Fattah-alhosseini, and M. Sabaghi Joni, J. Magnes. Alloy. 2 (2014) 175.

[20] A. Fattah-alhosseini, M. Sabaghi Joni, M.S. Joni, and M. Sabaghi Joni, J. Mater. Eng. Perform. 24 (2015) 3444.

[21] A. Fattah-alhosseini, and M.S. Joni, Int. J. Mater. Res. 106 (2015) 282.

[22] A. Fattah-alhosseini, and M.S. Joni, J. Alloys Compd. 646 (2015) 685.

[23] M. Sabaghi Joni, and A. Fattah-alhosseini, J. Alloys Compd. 661 (2016) 237.

[24] A. Fattah-alhosseini, and H. Asgari, Arab. J. Sci. Eng. 41 (2016) 169.

[25] A. Fattah-alhosseini, and H. Asgari, J. Mater. Eng. Perform. 27 (2018) 3248.

[26] J.E. Gray, and B. Luan, J. Alloys Compd. 336 (2002) 88.

[27] N. Yamauchi, K. Demizu, N. Ueda, N.K. Cuong, T. Sone, and Y. Hirose, Surf. Coatings Technol. 193 (2005) 277.

[28] K. Dong, Y. Song, D. Shan, and E.H. Han, Surf. Coatings Technol. 266 (2015) 188.

[29] G. Song, A. Atrens, X. Wu, and B. Zhang, Corros. Sci. 40 (1998) 1769.

[30] G. Barati Darband, M. Aliofkhazraei, P. Hamghalam, and N. Valizade, J. Magnes. Alloy 5 (2017) 74.

[31] L.J. Liu, and M. Schlesinger, Corros. Sci. 51 (2009) 1733.

[32] M. Pourbaix, Atlas of Electrochemical Equilibria in Aqueous Solutions Bokk, National Association of Corrosion; 2nd ed., Houston, 1974.

[33] M. Sabaghi Joni, A. Fattah-alhosseini, and M.J. Mahshid, Anal. Bioanal. Electrochem. 11 (2019) 448.

[34] A. Fattah-alhosseini, and S. Alizad, Anal. Bioanal. Electrochem. 7 (2015) 415.

[35] A. Fattah-alhosseini, M.K. Keshavarz, A. Masomi, and S. Marianaji, Egypt. J. Pet. 24 (2015) 405.

[36] A. Fattah-alhosseini, O. Imantalab, and F.R. Attarzadeh, J. Mater. Eng. Perform. 25 (2016) 4478.

[37] A. Fattah-alhosseini, M. Naseri, O. Imantalab, D. Gholami, and M. Haghshenas, J. Mater. Eng. Perform. 25 (2016) 4741.

[38] A. Fattah-alhosseini, and O. Imantalab, Anal. Bioanal. Electrochem. 8 (2016) 862.

[39] A. Fattah-alhosseini, O. Imantalab, F.R. Attarzadeh, and N. Attarzadeh, J. Mater. Eng. Perform. 26 (2017) 1634.

[40] D. Gholami, O. Imantalab, M. Naseri, S. Vafaeian, and A. Fattah-alhosseini, J. Alloys Compd. 723 (2017) 856.

[41] M. Naseri, D. Gholami, O. Imantalab, F.R. Attarzadeh, and A. Fattah-alhosseini, Mater. Res. Express. 5 (2018) 076504.

[42] A. Fattah-alhosseini, O. Ansari, and G. Imantalab, Anal. Bioanal. Electrochem. 10

(2018) 805.

[43] A. Fattah-alhosseini, O. Imantalab, and K. Babaei, Anal. Bioanal. Electrochem. 12 (2020) 107.

[44] A. Fattah-alhosseini, and O. Imantalab, J. Alloys Compd. 632 (2015) 48.

[45] O. Imantalab, and A. Fattah-alhosseini, J. Mater. Eng. Perform. 24 (2015) 2579.

[46] O. Imantalab, and A. Fattah-alhosseini, Anal. Bioanal. Electrochem. 7 (2015) 210.

[47] A. Fattah-alhosseini, A.H. Taheri, and M.K. Keshavarz, Trans. Indian Inst. Met. 69 (2016) 1423.

[48] O. Imantalab, A. Fattah-alhosseini, M.K. Keshavarz, and Y. Mazaheri, J. Mater. Eng. Perform. 25 (2016) 697.

[49] A. Fattah-alhosseini, and O. Imantalab, Metall. Mater. Trans. A. 47 (2016) 572.

[50] O. Imantalab, A. Fattah-alhosseini, Y. Mazaheri, and M.K. Keshavarz, Metall. Mater. Trans. A. 47 (2016) 3684.

[51] A. Fattah-alhosseini, O. Imantalab, and F.R. Attarzadeh, Metall. Mater. Trans. B. 47 (2016) 2761.

[52] J. Yang, Y. Li, and D.D. Macdonald, J. Nucl. Mater. 528 (2020) 151850.

[53] A. Fattah-alhosseini, M. Naseri, S.O. Gashti, S. Vafaeian, and M.K. Keshavarz, Corros. Sci. 131 (2018) 81.

[54] L.O. Osoba, A.M. Oladoye, and V.E. Ogbonna, J. Alloys Compd. 804 (2019) 376.

[55] A. Fattah-alhosseini, M. Naseri, S.O. Gashti, S. Vafaeian, and M.K. Keshavarz, J. Mater. Eng. Perform. 27 (2018) 3401.

[56] A. Fattah-alhosseini, Z. Masomi, and M. Mirzaei, Anal. Bioanal. Electrochem. 6 (2014) 646.

[57] A. Fattah-alhosseini, Arab. J. Sci. Eng. 40 (2015) 63.

[58] A. Fattah-alhosseini, A. Jalali, and S. Felegari, Arab. J. Sci. Eng. 40 (2015) 2985.

[59] A. Fattah-alhosseini, H. Aghamohammadi, and A.B. Safa, Anal. Bioanal. Electrochem. 7 (2015) 728.

[60] A. Fattah-alhosseini, A. Khodabandeloie, and M. Bahiraee, J. Mater. Environ. Sci. 7 (2016) 1128.

[61] A. Fattah-alhosseini, N. Rohani, F. Khodaei, Passive and electrochemical response of alloy 22 in alkaline solutions, Anal. Bioanal. Electrochem. 9 (2017) 174.

[62] N.P. Wasekar, N. Hebalkar, A. Jyothirmayi, B. Lavakumar, M. Ramakrishna, G. Sundararajan, Corros. Sci. (2019) 108409.

[63] F.J. Martin, G.T. Cheek, W.E. O'Grady, and P.M. Natishan, Corros. Sci. 47 (2005) 3187.

[64] S.O. Gashti, and A. Fattah-alhosseini, Anal. Bioanal. Electrochem. 6 (2014) 535.

[65] S.O. Gashti, A. Fattah-alhosseini, and Y. Mazaheri, Acta Metall. Sin. (English Lett. 29 (2016) 629.

[66] S.O. Gashti, A. Fattah-alhosseini, Y. Mazaheri, and M.K. Keshavarz, J. Manuf. Process. 22 (2016) 269.

[67] S.O. Gashti, A. Fattah-alhosseini, Y. Mazaheri, and M.K. Keshavarz, J. Alloys Compd. 688 (2016) 44.

[68] B. Zhang, Y. Li, and F. Wang, Corros. Sci. 52 (2010) 2612.

[69] L. Jinlong, L. Hongyun, and X. Jinpeng, Appl. Surf. Sci. 273 (2013) 192.

[70] A. Fattah-alhosseini, F.R. Attarzadeh, and M. Vakili-Azghandi, Metall. Mater. Trans. A. 48 (2017) 403.

[71] A. Fattah-alhosseini, M. Vakili-Azghandi, and M. Haghshenas, Int. J. Adv. Manuf. Technol. 90 (2017) 991.

[72] P. Jiang, J. Liang, and C. Lin, Appl. Surf. Sci. 280 (2013) 373.

[73] G. Ansari, and A. Fattah-alhosseini, Mater. Sci. Eng. C. 75 (2017) 64.

[74] A. Fattah-alhosseini, A.R. Ansari, Y. Mazaheri, and M.K. Keshavarz, Mater. Sci. Eng. C. 71 (2017) 771.

[75] A. Fattah-alhosseini, H. Elmkhah, and F.R. Attarzadeh, J. Mater. Eng. Perform. 26 (2017) 1792.

[76] F.R. Attarzadeh, H. Elmkhah, and A. Fattah-alhosseini, Metall. Mater. Trans. B. 48 (2017) 227.

[77] A. Fattah-alhosseini, M. Vakili-Azghandi, M. Sheikhi, and M.K. Keshavarz, J. Alloys Compd. 704 (2017) 499.

[78] A. Ebrahimi, H. Esfahani, A. Fattah-alhosseini, and O. Imantalab, J. Alloys Compd. 765 (2018) 826.

[79] A. Ebrahimi, H. Esfahani, A. Fattah-alhosseini, and O. Imantalab, J. Mater. Eng. Perform. 28 (2019) 1456.

[80] A. Fattah-alhosseini, O. Imantalab, and G. Ansari, Mater. Sci. Eng. C. 71 (2017) 827.

[81] A. Fattah-alhosseini, and S. Sharifi, Anal. Bioanal. Electrochem. 9 (2017) 862.

[82] F.R. Attarzadeh, N. Attarzadeh, S. Vafaeian, and A. Fattah-alhosseini, J. Mater. Eng. Perform. 25 (2016) 4199.

[83] A. Fattah-alhosseini, F.R. Attarzadeh, S. Vafaeian, M. Haghshenas, and M.K. Keshavarz, Int. J. Refract. Met. Hard Mater. 64 (2017) 168.

[84] A. Fattah-alhosseini, and M. Pourmahmoud, J. Mater. Eng. Perform. 27 (2018) 116.

[85] A. Fattah-alhosseini, H. Elmkhah, G. Ansari, F. Attarzadeh, and O. Imantalab, J. Alloys Compd. 739 (2018) 918.

[86] A. Fattah-alhosseini, H. Elmkhah, K. Babaei, O. Imantalab, H.R. Ghomi, and M.K. Keshavarz, Mater. Res. Express. 5 (2018) 106401.

[87] A. Fattah-alhosseini, M. Roknian, and K. Babaei, Mater. Res. Express. 5 (2018) 116514.

[88] A. Fattah-alhosseini, S. Vafaeian, A.R. Ansari, and M. Khanmohammadi, Anal.

Bioanal. Electrochem. 9 (2017) 660.
[89] A.M. Oje, A.A. Ogwu, S.U. Rahman, A.I. Oje, and N. Tsendzughul, Corros. Sci. 154 (2019) 28.
[90] D.S. Kong, S.H. Chen, C. Wang, and W. Yang, Corros. Sci. 45 (2003) 747.
[91] C. Boissy, B. Ter-Ovanessian, N. Mary, and B. Normand, Electrochim. Acta. 174 (2015) 430.
[92] A. Fattah-alhosseini, and M. Mirshekari, Trans. Indian Inst. Met. 68 (2015) 851.
[93] T. Kaewmaneekul, and G. Lothongkum, Corros. Sci. 66 (2013) 67.
[94] J.R. Vilche, K. Jüttner, W.J. Lorenz, W. Kautek, W. Paatsch, M.H. Dean, and U. Stimming, Corros. Sci. 31 (1990) 679.
[95] A. Bohe, J. Vilche, K. Jüttner, W. Lorenz, W. Kautek, and W. Paatasch, Corros. Sci. 32 (1991) 621.
[96] M. Uno, M. Okui, K. Kurosaki, S. Yamanaka, K. Takeda, and Y. Ishii, J. Alloys Compd. 368 (2004) 18.
[97] A. Fattah-alhosseini, and N. Attarzadeh, Anal. Bioanal. Electrochem. 7 (2015) 254.
[98] T. Nishizaki, M. Okui, K. Kurosaki, M. Uno, S. Yamanaka, K. Takeda, and H. Anada, J. Alloys Compd. 330–332 (2002) 307.
[99] S. Ahn, and H. Kwon, J. Electroanal. Chem. 579 (2005) 311.
[100] Y. Zhao, T. Pan, X. Yu, and D. Chen, Corros. Sci. 158 (2019) 108097.
[101] P.M. Samim, and A. Fattah-alhosseini, Anal. Bioanal. Electrochem. 8 (2016) 644.
[102] G.A. Zhang, and Y.F. Cheng, Electrochim. Acta. 55 (2009) 316.
[103] D.G. Li, Y.R. Feng, Z.Q. Bai, J.W. Zhu, and M.S. Zheng, Appl. Surf. Sci. 254 (2008) 2837.
[104] I.M. Gadala, and A. Alfantazi, Appl. Surf. Sci. 357 (2015) 356.
[105] S. Ningshen, U. Kamachi Mudali, V.K. Mittal, and H.S. Khatak, Corros. Sci. 49 (2007) 481.
[106] L. Zeng, X.P. Guo, G.A. Zhang, and H.X. Chen, Corros. Sci. 144 (2018) 258.
[107] J. Yao, D.D. Macdonald, and C. Dong, Corros. Sci. 146 (2019) 221.
[108] A. Fattah-alhosseini, and S. Vafaeian, Egypt. J. Pet. 24 (2015) 333.
[109] A. Fattah-alhosseini, and S. Vafaeian, J. Alloys Compd. 639 (2015) 301.
[110] A. Fattah-alhosseini, and S. Vafaeian, J. Mater. Res. Technol. 4 (2015) 423.
[111] A. Fattah-alhosseini, and S. Vafaeian, Appl. Surf. Sci. 360 (2016) 921.
[112] S. Vafaeian, A. Fattah-alhosseini, M.K. Keshavarz, and Y. Mazaheri, J. Alloys Compd. 677 (2016) 42.
[113] P.M. Samim, and A. Fattah-alhosseini, Anal. Bioanal. Electrochem. 8 (2016) 717.
[114] S. Vafaeian, A. Fattah-alhosseini, M.K. Keshavarz, and Y. Mazaheri, J. Mater. Eng. Perform. 26 (2017) 676.
[115] F. Qods, S. Maryanaji, A. Fattah-alhosseini, and B. Electrochemistry, Anal. Bioanal.

Electrochem. 10 (2018) 161.
[116] D.D. MacDonald, Electrochim. Acta. 56 (2011) 1761.
[117] Z. Lu, and D.D. Macdonald, Electrochim. Acta. 53 (2008) 7696.
[118] D.D. Macdonald, J. Electrochem. Soc. 153 (2006) B213.
[119] D.D. Macdonald, J. Nucl. Mater. 379 (2008) 24.
[120] A. Fattah-alhosseini, and O. Imantalab, Anal. Bioanal. Electrochem. 8 (2016) 862.
[121] A. Fattah-alhosseini, A.R. Ansari, Y. Mazaheri, and M. Karimi, J. Mater. Eng. Perform. 26 (2017) 611.
[122] R. Khatami, A. Fattah-alhosseini, and M.K. Keshavarz, J. Alloys Compd. 708 (2017) 316.
[123] M.K. Keshavarz, and A. Fattah-alhosseini, Arab. J. Chem. 13 (2018) 1858.
[124] T. Zhang, Y. Shao, G. Meng, Y. Li, and F. Wang, Electrochim. Acta. 52 (2006) 1323.
[125] T. Zhang, Y. Li, and F. Wang, Corros. Sci. 48 (2006) 1249.
[126] R.A. Antunes, M.C.L. de Oliveira, and I. Costa, Mater. Corros. (2011) doi.org/10.1002/maco.201006052.
[127] H. Duan, C. Yan, and F. Wang, Electrochim. Acta. 52 (2007) 3785.
[128] M.J. Carmezim, A.M. Simões, M.O. Figueiredo, and M. Da Cunha Belo, Corros. Sci. 44 (2002) 451.
[129] G. Goodlet, S. Faty, S. Cardoso, P. Freitas, A.M. Simões, M.G. Ferreira, and M. Da Cunha Belo, Corros. Sci. 46 (2004) 1479.
[130] S. Maximovitch, Electrochim. Acta. 41 (1996) 2761.
[131] K. Azumi, J. Electrochem. Soc. 134 (1987) 1352.
[132] A. Frichet, P. Gimenez, and M. Keddam, Electrochim. Acta. 38 (1993) 1957.
[133] T.M. Silva, A.M.P. Simões, M.G.S. Ferreira, M. Walls, and M. Da Cunha Belo, J. Electroanal. Chem. 441 (1998) 5.